

# NATIONAL TRANSPORTATION SAFETY BOARD

Office of Research and Engineering  
Materials Laboratory Division  
Washington, D.C. 20594



April 15, 2021

MATERIALS LABORATORY FACTUAL REPORT

Report No. 21-034

## A. ACCIDENT INFORMATION

Place : Anchorage, Alaska  
Date : June 8, 2020  
Vehicle : Piper PA-12  
NTSB No. : ANC20LA059  
Investigator : Brice Banning, AS-ANC

## B. COMPONENTS EXAMINED

Exemplar fractured rudder post from a Piper PA-18 airplane.

## C. DETAILS OF THE EXAMINATION

An overall view of the submitted rudder post pieces is shown in figure 1. The rudder was from a Piper PA-18 airplane and was submitted as an exemplar fractured rudder post in support of the accident investigation described in Section A above. The rudder post was fractured approximately 1.31 inches above the upper hinge barrel, and the submitted pieces had been cut from the remainder of the rudder to facilitate shipment and examination at the NTSB Materials Laboratory.

A photograph of the fracture surface on the lower piece is shown at the lower right in figure 1. The fracture surfaces on both sides of the fracture were substantially battered and rubbed with post-fracture contact between the mating fracture surfaces. The tubular cross-section of the post was deformed into an oblong shape at the fracture location with flattening on both the left and right sides, but the left side was flattened more, resulting in a cross-section that resembled a "D" shape.

Transverse cuts were made through the post near the fracture surfaces, and the pieces with fracture surfaces were submerged in a solution of Alconox detergent and water and cleaned using an ultrasonic cleaner. The sectioned and cleaned pieces with the upper and lower sides of the fracture are shown in figure 2. Most of the fracture occurred in a nearly circumferential plane with a relatively large step on the right side. A circumferential branching crack was observed at the location of the step, and another nearly longitudinal branching crack was observed nearby as indicated with brackets in the upper image in figure 2. Rubbing deformation on the fracture surface and relative displacement of the branching crack faces were consistent with final fracture at the right side between the branching cracks with the upper side of the fracture rotating clockwise relative to the lower side (clock references as viewed from above).

---

The piece with the lower fracture surface was examined using a scanning electron microscope (SEM). Most of the fracture surface was rubbed, obliterating the original fracture features. However, isolated areas with fracture features were observed in the left aft quadrant of the fracture surface including the area shown in figure 3. Flat fracture features with curving striations were observed consistent with a fatigue fracture mechanism. Unlabeled arrows in figure 3 indicate the direction of fatigue crack propagation at this location, consistent with circumferential fatigue crack growth in a counterclockwise direction.

The skin on the lower piece was peeled from the surface, and a piece of the rudder post was cut from the lower end of the lower piece to facilitate dimensional measurements at a location approximately 2.5 inches below the upper hinge barrel. The exterior coatings were scraped from portions of the surface using a scalpel, and oxides on the interior surface were lightly sanded using 600-grit silicon carbide paper. The outside diameter of the tube measured 0.8883 inch forward to aft and 0.8675 inch side to side. The wall thickness measured 0.0385 inch.

The exterior surface of the section cut from the lower end of the post piece was further ground with varying grit sizes of silicon carbide paper up to 600 grit to remove surface layers in preparation for compositional analysis and hardness testing. The composition was analyzed using an Olympus Vanta x-ray fluorescence (XRF) alloy analyzer and was identified as carbon steel consistent with AISI 1025 carbon steel originally specified for use in the rudder post until the material was changed to AISI 4130 low alloy steel in a Piper engineering change order dated June 3, 1974.

Hardness was measured on the exterior surface of the post piece. The average hardness measured 53.6 HR30TW (including curvature compensation of 0.6 added to the measured values in accordance with ASTM standard E18).<sup>1</sup> The measured hardness corresponded to 55.9 HRB as converted using a table in ASTM standard A370.<sup>2</sup> An approximate tensile strength is not associated with this hardness value in ASTM Standard A370 where a hardness of 65 HRB corresponds to a tensile strength of 56 ksi. The Air Force – Navy – Commerce Bulletin ANC-5 lists properties for alloy 1025 steel tube, and the ultimate tensile strength for general design purposes is listed as 55 ksi.<sup>3</sup>

Matthew R. Fox, Ph.D.  
Senior Materials Engineer

---

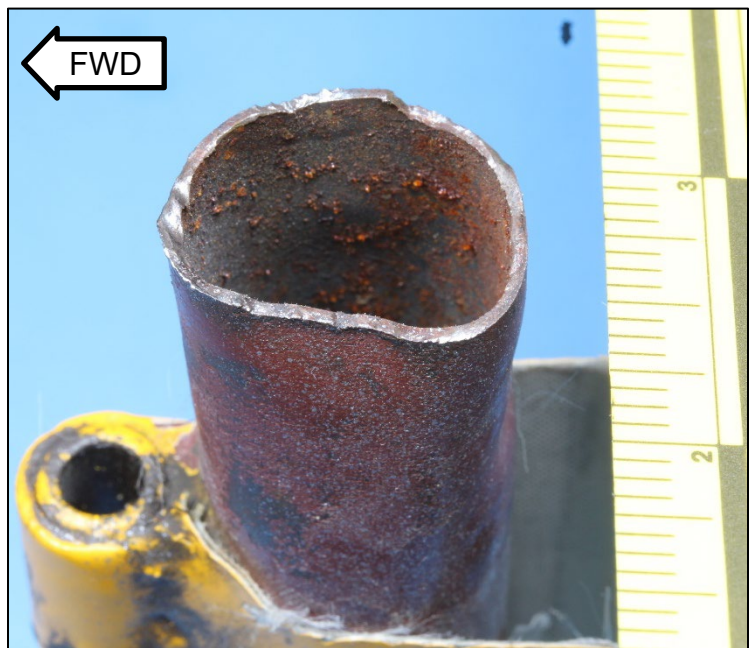
<sup>1</sup> ASTM Standard E18-20, *Standard Test Methods for Rockwell Hardness of Metallic Materials*, ASTM International, West Conshohocken, PA, 2020, [www.astm.org](http://www.astm.org)

<sup>2</sup> ASTM Standard A370-19e1, *Standard Test Methods and Definitions for Mechanical Testing of Steel Products*, ASTM International, West Conshohocken, PA, 2019, [www.astm.org](http://www.astm.org)

<sup>3</sup> Air Force – Navy – Commerce Bulletin ANC-5, *Strength of Metal Aircraft Elements*, US Department of Defense (1951).



Figure 1. Overall view of the submitted rudder post pieces (left) with a closer look at the fracture surface on the lower piece (below).



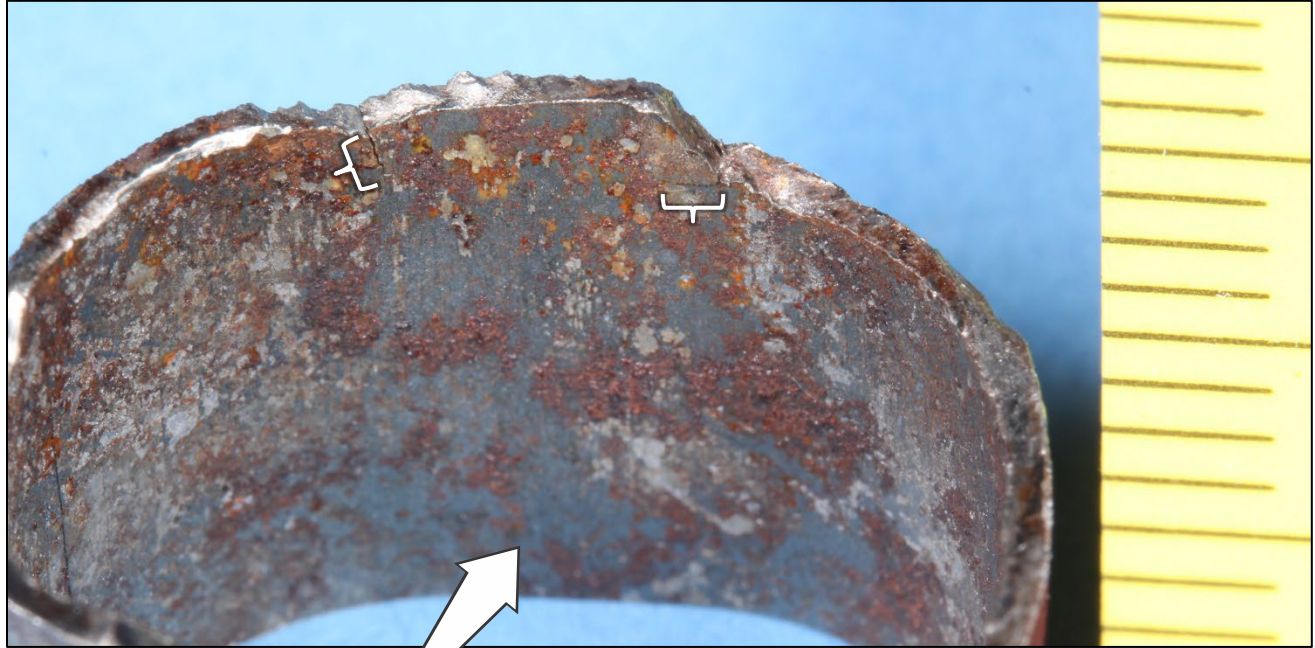


Figure 2. Upper and lower sides of the fracture after sectioning and cleaning (left) with a closer view of the right side of the lower fracture surface (above). Brackets in the upper image indicate branching cracks.

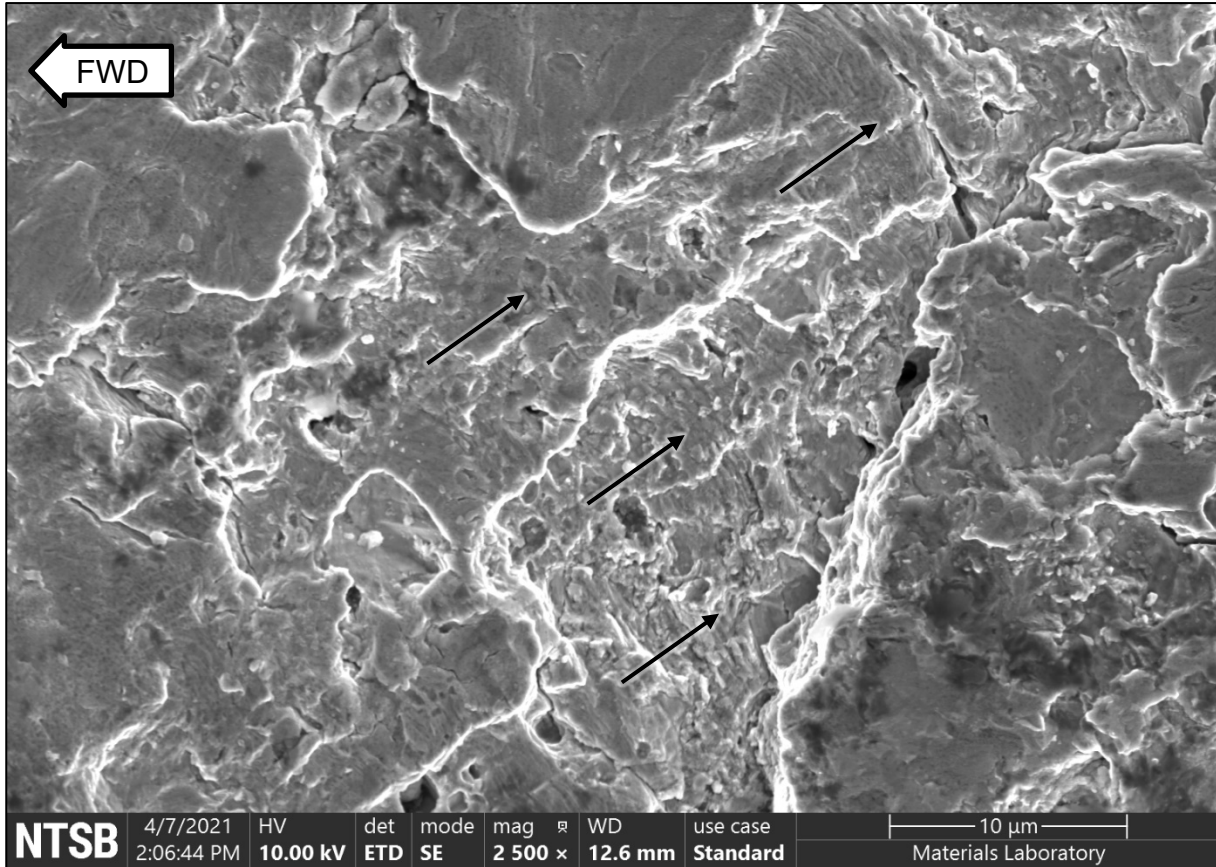


Figure 3. SEM image of fatigue fracture features on the lower piece. The area shown was in the aft left quadrant, and unlabeled arrows indicate the direction of circumferential fatigue crack propagation.